

An efficient and Long-Time Accurate Third-Order Algorithm for the Stokes-Darcy System

Wenbin Chen · Max Gunzburger · Dong Sun · Xiaoming Wang

Received: date / Accepted: date

Abstract A third-order in time numerical IMEX-type algorithm for the Stokes-Darcy system for flows in fluid saturated karst aquifers is proposed and analyzed. A novel third-order Adams-Moulton scheme is used for the discretization of the dissipative term whereas a third-order explicit Adams-Bashforth scheme is used for the time discretization of the interface term that couples the Stokes and Darcy components. The scheme is efficient in the sense that one needs to solve, at each time step, decoupled Stokes and Darcy problems. Therefore, legacy Stokes and Darcy solvers can be applied in parallel. The scheme is also unconditionally stable and, with a mild time-step restriction, long-time accurate in the sense that the error is bounded uniformly in time. Numerical experiments are used to illustrate the theoretical results. To the authors' knowledge, the novel algorithm is the first third-order accurate numerical scheme for the Stokes-Darcy system possessing its favorable efficiency, stability, and accuracy properties.

This work is supported in part by a grant from the NSF.

Wenbin Chen
School of Mathematical Sciences, Fudan University
E-mail: wbchen@fudan.edu.cn

Max Gunzburger
Department of Scientific Computing, Florida State University
E-mail: gunzburg@fsu.edu

Dong Sun
Department of Mathematics, Florida State University
E-mail: dsun@math.fsu.edu

Xiaoming Wang
Department of Mathematics, Florida State University
E-mail: wxm@math.fsu.edu *Corresponding author*

Keywords Stokes-Darcy system · Adams-Moulton-Bashforth method · unconditional stability · uniform in time error estimates · third-order accurate in time · karst aquifers

Mathematics Subject Classification (2000) 35M13 · 35Q35 · 65N30 · 65N55 · 76D07 · 76S05

1 Introduction

Certain rocks such as limestone, dolomite and gypsum are susceptible to dissolution due to reaction with carbon-dioxide and water which leads, over long (geological) time, to the formation of voids (vugs) and conduits. This type of landscape is referred to as karst. Due to the existence of vugs and conduits, large amount of water may be stored in karst regions to form karst aquifers that are of great practical importance and are susceptible to pollution [34]. For example, about 90% of the fresh water used in the State of Florida comes from karst aquifers and contamination is a serious problem [32].

For many important applications such as contaminant transport in karst aquifers, one must couple the fluid motion in the porous media with the fluid motion in the conduit or vugs. For instance, contaminants driven into the porous media during a flood season may be released during a drought season. Moreover, because fluid motion in the porous media (matrix) is much slower compared to fluid motion in conduits, long-time accurate numerical schemes are highly desirable if one is interested in capturing the physically interesting retention and release of contaminants within karst aquifers.

There has been a recent surge in interest in the design and analysis of numerical algorithms for the Stokes-Darcy and related systems that govern the motion of fluids flows in saturated karst aquifers. See, e.g., [9–11, 14–16, 19–23, 25, 33, 35–42, 45–48]. In particular, first order and second order in time accurate and long-time stable schemes have been proposed and studied in [11, 16, 36, 37, 42].

The purpose of this work is to propose and investigate a novel third-order Adams-Moulton-Bashforth method for the Stokes-Darcy system. The algorithm is a special case of the implicit-explicit (IMEX) class of schemes [1–3, 5]. The coupling term in the interface conditions is treated explicitly in our algorithm so that only two decoupled problems (one Stokes and one Darcy) are solved at each time step. Therefore, the scheme can be implemented very efficiently and, in particular, legacy codes for each of the two components can be utilized. Moreover, we show that our scheme is unconditionally stable and long-time stable in the sense that the solutions remain bounded uniformly in time. The uniform in time bound of the solutions further leads to uniform in time error estimates. This is a highly desirable feature because one would want to have reliable numerical results over the long-time scale of contaminant sequestration and release. We also provide the results of numerical experiments that illustrate our analytical results.

38 This work can be viewed as an improvement of our earlier work [16] in
 39 which a second-order in time Adams-Moulton-Bashforth algorithm was stud-
 40 ied. This is the first third-order algorithm that is unconditionally stable, long-
 41 time accurate in the sense of the existence of a uniform-in-time error bound,
 42 and efficient in the sense that only two decoupled problems (one Stokes, one
 43 Darcy) are needed at each time step.

44 The rest of the paper is organized as follows. In Section 2, we introduce the
 45 coupled Stokes-Darcy system, the associated weak formulation, and the third-
 46 order in time scheme. The unconditional and long-time stability with respect
 47 to the L^2 norm are presented in Section 3. Numerical results that illustrate
 48 the accuracy, efficiency, and long-time stability of our algorithms are given in
 49 Section 4. We close by providing some concluding remarks in Section 5.

50 2 The Stokes-Darcy system and one type of third order IMEX 51 method

52 In this section we recall the Stokes-Darcy system modeling flows in saturated
 53 karst aquifers. A third-order in time numerical scheme based on the Adams-
 54 Moulton-Bashforth approach is presented as well.

55 *The Stokes-Darcy system.* For simplicity, the following conceptual domain is
 56 considered for a karst aquifer. It contains a porous media (matrix), denoted
 57 by $\Omega_p \in \mathbb{R}^d$, and a conduit, denoted by $\Omega_f \in \mathbb{R}^d$, where $d = 2, 3$ denotes the
 58 spatial dimension. Γ denotes the interface between the matrix and the conduit.
 59 The remaining pieces of the boundaries for the matrix and the conduit are
 60 denoted $\partial\Omega_p$ and $\partial\Omega_f$, respectively. We assume $\partial\Omega_p$ and $\partial\Omega_f$ are non-empty
 61 for simplicity.

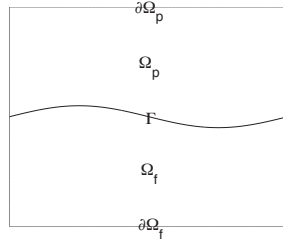


Fig. 1 The physical domain consisting of a porous media Ω_p and a free-flow conduit Ω_f .

The governing coupled Stokes-Darcy system for karst aquifers is given by

$$\begin{cases} S \frac{\partial \phi}{\partial t} - \nabla \cdot (\mathbb{K} \nabla \phi) = f & \text{in } \Omega_p, \\ \frac{\partial \mathbf{u}_f}{\partial t} - \frac{1}{\rho} \nabla \cdot \mathbb{T}(\mathbf{u}_f, p) = \mathbf{f} \quad \text{and} \quad \nabla \cdot \mathbf{u}_f = 0 & \text{in } \Omega_f, \end{cases} \quad (1)$$

where the unknowns are the hydraulic head ϕ in the matrix and the fluid velocity \mathbf{u}_f and the pressure p in the conduit [18]. The Darcy velocity \mathbf{u}_p in the matrix can be recovered by the Darcy equation $\mathbf{u}_p = -\mathbb{K}\nabla\phi$. In (1), f denotes a sink or source in the matrix, \mathbf{f} denotes a body force density in the conduit, ρ the fluid density which is taken to be 1 for simplicity, and $\mathbb{T}(\mathbf{u}_f, p)$ denotes the stress tensor in the conduit. The physical parameters involved are the water storage coefficient S , the hydraulic conductivity tensor \mathbb{K} , and the kinematic viscosity of the fluid ν . For simplicity, we assume homogeneous Dirichlet boundary conditions for the hydraulic head ϕ and the free flow velocity \mathbf{u}_f in the conduit except on the interface Γ . On the interface Γ , we impose the continuity of normal velocity (for conservation of mass), the balance of normal component of the normal stress, and the Beavers-Joseph-Saffman-Jones interface boundary conditions (BJSJ) [6, 31, 44]:

$$\begin{cases} \mathbf{u}_f \cdot \mathbf{n}_f = \mathbf{u}_p \cdot \mathbf{n}_f = -(\mathbb{K}\nabla\phi) \cdot \mathbf{n}_f \\ -\boldsymbol{\tau}_j \cdot (\mathbb{T}(\mathbf{u}_f, p_f) \cdot \mathbf{n}_f) = \alpha_{BJSJ} \boldsymbol{\tau}_j \cdot \mathbf{u}_f, \quad j = 1, \dots, d-1 \\ -\mathbf{n}_f \cdot (\mathbb{T}(\mathbf{u}_f, p_f) \cdot \mathbf{n}_f) = g\phi. \end{cases} \quad (2)$$

⁶² In (2), \mathbf{n}_f denotes the outer normal vector to Ω_f and $\{\boldsymbol{\tau}_j\}$, $j = 1, 2, \dots, d-1$,
⁶³ denotes a set of linearly-independent tangential vectors on the interface Γ .
⁶⁴ The additional physical parameters are the gravitational constant g and the
⁶⁵ Beavers-Joseph-Saffman-Jones coefficient $\alpha_{BJSJ} = \frac{\bar{\alpha}_{BJSJ}\sqrt{d\nu}}{\sqrt{\text{trace}(\mathbb{K})}}$.

Weak formulation of the Stokes-Darcy system. Let $(\cdot, \cdot)_D$ and $\|\cdot\|_D$ denote the standard $L^2(D)$ inner product and norm, respectively, where D can be Ω_p , Ω_f , or Γ . We omit D whenever there is no ambiguity. We define the function spaces

$$\begin{aligned} \mathbf{H}_f &= \left\{ \mathbf{v} \in (H^1(\Omega_f))^d \mid \mathbf{v} = \mathbf{0} \text{ on } \partial\Omega_f \setminus \Gamma \right\}, \\ H_p &= \left\{ \psi \in H^1(\Omega_p) \mid \psi = 0 \text{ on } \partial\Omega_p \setminus \Gamma \right\}, \\ Q &= L^2(\Omega_f), \quad \mathbf{W} = \mathbf{H}_f \times H_p. \end{aligned}$$

⁶⁶ Let X' denote the dual space of X with respect to the duality induced by
⁶⁷ the L^2 inner product. The X', X action is denoted by $\langle \cdot, \cdot \rangle_{X', X}$ with the
⁶⁸ subscript omitted if it is clear from the context.

A weak formulation of the Stokes-Darcy system is then derived by the following procedure. First, we multiply the three equations in (1) by three test functions $\mathbf{v} \in \mathbf{H}_f$, $g\psi \in H_p$, and $q \in Q$, respectively, and integrate the results over each corresponding domain. Then, integration by parts is applied to the terms involving second order derivatives, a process that produces boundary integrals. Finally, we appropriately substitute the BJSJ interface boundary conditions (2) into the boundary integral terms to arrive at the weak formulation

$$\begin{aligned} \langle \langle \mathbf{u}_t, \mathbf{v} \rangle \rangle + a(\mathbf{u}, \mathbf{v}) + b(\mathbf{v}, p) + a_\Gamma(\mathbf{u}, \mathbf{v}) &= \langle \mathbf{f}, \mathbf{v} \rangle \quad \forall \mathbf{v} \in \mathbf{W}, \\ b(\mathbf{u}, q) &= 0 \quad \forall q \in Q, \end{aligned} \quad (3)$$

where $\mathbf{W} = \mathbf{H}_f \times H_p$, $\mathbf{u} = [\mathbf{u}, \phi]^T$, $\mathbf{v} = [\mathbf{v}, \psi]^T$, $\mathbf{f} = [\mathbf{f}, gf]^T$, $(\cdot)_t = \partial(\cdot)/\partial t$,

$$\begin{aligned} \langle \langle \mathbf{u}_t, \mathbf{v} \rangle \rangle &= \langle \mathbf{u}_t, \mathbf{v} \rangle_{\Omega_f} + gS \langle \phi_t, \psi \rangle_{\Omega_p}, & b(\mathbf{v}, q) &= -(q, \nabla \cdot \mathbf{v})_{\Omega_f}, \\ a(\mathbf{u}, \mathbf{v}) &= a_f(\mathbf{u}, \mathbf{v}) + a_p(\phi, \psi) + a_{BJSJ}(\mathbf{u}, \mathbf{v}), \\ a_\Gamma(\mathbf{u}, \mathbf{v}) &= g(\phi, \mathbf{v} \cdot \mathbf{n}_f)_\Gamma - g(\mathbf{u} \cdot \mathbf{n}_f, \psi)_\Gamma, \\ \langle \langle \mathbf{f}, \mathbf{v} \rangle \rangle &= \langle \mathbf{f}, \mathbf{v} \rangle_{\Omega_f} + \langle gf, \psi \rangle_{\Omega_p}, \end{aligned} \quad (4)$$

with

$$\begin{aligned} a_f(\mathbf{u}, \mathbf{v}) &= \nu(\nabla \mathbf{u}, \nabla \mathbf{v})_{\Omega_f}, & a_p(\phi, \psi) &= g(\mathbb{K} \nabla \phi, \nabla \psi)_{\Omega_p} \\ a_{BJSJ}(\mathbf{u}, \mathbf{v}) &= \alpha_{BJSJ}(\mathbf{u} \cdot \boldsymbol{\tau}, \mathbf{v} \cdot \boldsymbol{\tau})_\Gamma. \end{aligned}$$

The bilinear form $a(\cdot, \cdot)$ can be shown to be coercive, i.e.,

$$a(\mathbf{u}, \mathbf{u}) \geq (\nu \|\nabla \mathbf{u}\|^2 + gK_{\min} \|\nabla \phi\|^2 + \alpha_{BJSJ} \|\mathbf{u} \cdot \boldsymbol{\tau}\|_\Gamma^2) \geq C_a \|\nabla \mathbf{u}\|^2, \quad (5)$$

69 where $C_a = \min(\nu, gK_{\min}) > 0$ and K_{\min} denotes the smallest eigenvalue of
70 \mathbb{K} . Details can be found in, e.g., [8, 16].

For the sake of exposition, we introduce the two norms

$$\|\mathbf{u}\|_a = (a(\mathbf{u}, \mathbf{u}))^{\frac{1}{2}}, \quad \|\mathbf{v}\|_S = (\langle \langle \mathbf{v}, \mathbf{v} \rangle \rangle)^{\frac{1}{2}}.$$

It is easy to see that $\|\mathbf{v}\|_S$ is equivalent to the L^2 norm, i.e.,

$$C_s \|\mathbf{v}\|_S \leq \|\mathbf{v}\| \leq C_S \|\mathbf{v}\|_S, \quad (6)$$

71 where $C_s = \min\{1, \sqrt{gS}\}$ and $C_S = \max\{1, \sqrt{gS}\}$.

Third-order Adams-Moulton-Bashforth IMEX method (AMB3). To define our novel third-order scheme that is unconditionally stable and long-time accurate, we first define two Adams-type difference operators. The first is the novel Adams-Moulton difference operator defined on a $2\Delta t$ mesh

$$D_{AM}v^{n+1} = \frac{2}{3}v^{n+1} + \frac{5}{12}v^{n-1} - \frac{1}{12}v^{n-3}, \quad (7)$$

and the other is the Adams-Bashforth difference operator

$$D_{AB}v^{n+1} = \frac{23}{12}v^n - \frac{4}{3}v^{n-1} + \frac{5}{12}v^{n-2}. \quad (8)$$

72 Note that the Adams-Moulton operator (7) is different from the standard one
73 $\frac{5}{12}v^{n+1} + \frac{2}{3}v^n - \frac{1}{12}v^{n-1}$. The novel form of the Adams-Moulton operator that
74 we adopt here is, due to its dissipativity, crucial to the long-time stability.

The third-order Adams-Moulton-Bashforth method is a combination of the third-order explicit Adams-Bashforth treatment for the coupling term and the novel third-order Adams-Moulton method for the remaining terms. Specifically, we have, for any $\mathbf{v} \in \mathbf{W}$ and $q \in Q$,

$$\begin{aligned} \left\langle \left\langle \frac{\mathbf{u}^{n+1} - \mathbf{u}^n}{\Delta t}, \mathbf{v} \right\rangle \right\rangle &+ \tilde{a}(D_{AM}\mathbf{u}^{n+1}, \mathbf{v}) + b(\mathbf{v}, D_{AM}p^{n+1}) \\ &= \langle D_{AM}\mathbf{f}^{n+1}, \mathbf{v} \rangle - \tilde{a}_\Gamma(D_{AB}\mathbf{u}^{n+1}, \mathbf{v}), \\ b(D_{AM}\mathbf{u}^{n+1}, q) &= 0. \end{aligned} \quad (9)$$

Here the bilinear form $\tilde{a}(\mathbf{u}, \mathbf{v})$ is defined as

$$\tilde{a}(\mathbf{u}, \mathbf{v}) = a(\mathbf{u}, \mathbf{v}) + a_{st}(\mathbf{u}, \mathbf{v}),$$

where the artificial stabilizing term $a_{st}(\cdot, \cdot)$ is defined as

$$a_{st}(\mathbf{u}, \mathbf{v}) = \gamma_f(\mathbf{u} \cdot \mathbf{n}_f, \mathbf{v} \cdot \mathbf{n}_f)_\Gamma + \gamma_p(\phi, \psi)_\Gamma \quad (10)$$

with parameters $\gamma_f, \gamma_p \geq 0$. It is obvious that

$$\tilde{a}(\mathbf{u}, \mathbf{u}) \geq a(\mathbf{u}, \mathbf{u}) \geq C_a \|\nabla \mathbf{u}\|^2, \quad (11)$$

so that we can define the norm

$$\|\mathbf{u}\|_a^2 = \tilde{a}(\mathbf{u}, \mathbf{u}).$$

The interface term $a_\Gamma(\mathbf{u}, \mathbf{v})$ is modified by $\tilde{a}_\Gamma(\mathbf{u}, \mathbf{v})$ as

$$\tilde{a}_\Gamma(\mathbf{u}, \mathbf{v}) = a_\Gamma(\mathbf{u}, \mathbf{v}) - a_{st}(\mathbf{u}, \mathbf{v}).$$

Efficiency of the scheme. Note that the only term that couples the Stokes equation in the conduit with the equation in the matrix is the interface term \tilde{a}_Γ through a_Γ . Because this coupling term is treated explicitly in our scheme (9), the scheme is of high efficiency because we only need to solve two decoupled subproblems at each time step, one Stokes and one Darcy:

1. At time $t = t_{n+1}$, given $\mathbf{u}^n, \mathbf{u}^{n-1}, \mathbf{u}^{n-2}, \mathbf{u}^{n-3}$;
2. Set $\mathbf{v} = [\mathbf{v}, 0]$ so that all the terms involving ϕ^{n+1} vanish and thus we only need apply a fast Stokes solver to determine \mathbf{u}^{n+1} ;
3. Set $\mathbf{v} = [\mathbf{0}, g\psi]$ so that all the terms involving \mathbf{u}^{n+1} vanish and thus we only need apply a fast Darcy solver for ϕ^{n+1} ;
4. Set $n = n + 1$ and return to step 1.

The computation of step 2 and 3 can be conducted in a parallel fashion and one can use legacy Stokes and Darcy codes, respectively, for each step, if one so desires.

3 Unconditional and long-time stability

Useful inequalities. We recall a few inequalities to aid readability.

– Trace inequality: if $\mathbf{v} \in \mathbf{W}$, then

$$\|\mathbf{v}\|_\Gamma \leq C_{tr} \sqrt{\|\mathbf{v}\| \|\nabla \mathbf{v}\|}, \quad \|\mathbf{v}\|_\Gamma \leq C_{tr} \|\nabla \mathbf{v}\|, \quad \|\mathbf{v}\|_\Gamma \leq C_{tr} \|\mathbf{v}\|_{\tilde{a}}. \quad (12)$$

– Poincaré inequality: if $\mathbf{v} \in \mathbf{W}$, then

$$\|\mathbf{v}\| \leq C_P \|\nabla \mathbf{v}\|. \quad (13)$$

– Young inequality:

$$a^{\frac{1}{2}} b^{\frac{1}{2}} c \leq \frac{a^2}{64\varepsilon^3} + \varepsilon(b^2 + c^2) \quad \forall a, b, c, \varepsilon > 0. \quad (14)$$

– Triangle inequality: $\|a + b\|^{\frac{1}{2}} \leq \|a\|^{\frac{1}{2}} + \|b\|^{\frac{1}{2}}$.

Other variants of Young's inequality will also be used.

93 *Useful lemmas.* Here we introduce a few useful lemmas that are useful in the
94 analysis of our schemes.

95 The following estimates follow from the basic inequalities.

Lemma 1 *Let $a_\gamma(\cdot, \cdot)$ and $a_{st}(\cdot, \cdot)$ be defined as in (4) and (10), respectively. Then, there exists a constant C_{ct} such that*

$$|\tilde{a}_\Gamma(\mathbf{u}, \mathbf{v})| \leq |a_{st}(\mathbf{u}, \mathbf{v})| + |a_\Gamma(\mathbf{u}, \mathbf{v})| \leq C_{ct} \|\mathbf{u}\|_\Gamma \|\mathbf{v}\|_\Gamma \quad \forall \mathbf{u}, \mathbf{v} \in \mathbf{W}.$$

Lemma 2 *For any $\beta_1 > 0$, $\mathbf{v}, \mathbf{w} \in \mathbf{W}$, we have*

$$|\tilde{a}_\Gamma(\mathbf{v}, \mathbf{w})| \leq \beta_1 (\|\mathbf{v}\|_a^2 + \|\mathbf{w}\|_a^2) + \beta_2 \|\mathbf{v}\|_S^2, \quad (15)$$

96 where $\beta_2 = \frac{1}{64} \beta_1^{-3} C_S^2 C_{ct}^4 C_{tr}^8 C_a^{-1}$.

Proof By Lemma 1, the equivalence between $\|\cdot\|_S$ and $\|\cdot\|$, (6), (11), and the trace theorem, we have, for any $\mathbf{v}, \mathbf{w} \in \mathbf{W}$,

$$\begin{aligned} \tilde{a}_\Gamma(\mathbf{v}, \mathbf{w}) &\leq C_{ct} \|\mathbf{v}\|_\Gamma \|\mathbf{w}\|_\Gamma \leq C_{ct} C_{tr}^2 \|\mathbf{v}\|^{1/2} \|\nabla \mathbf{v}\|^{1/2} \|\mathbf{w}\|_{\tilde{a}} \\ &\leq C_S^{1/2} C_{ct} C_{tr}^2 C_a^{-1/4} \|\mathbf{v}\|_S^{1/2} \|\mathbf{v}\|_a^{1/2} \|\mathbf{w}\|_{\tilde{a}}. \end{aligned} \quad (16)$$

97 The inequality (15) is then obtained by setting $\varepsilon = \beta_1 C_S^{-1/2} C_{ct}^{-1} C_{tr}^{-2} C_a^{1/4}$ in the
98 Young's inequality.

Lemma 3 *The interface term $\tilde{a}_\Gamma(D_{AB}\mathbf{u}, \mathbf{u})$ can be bounded by*

$$\begin{aligned} &-2\Delta t \tilde{a}_\Gamma \left(\frac{23}{12} \mathbf{u}^n - \frac{4}{3} \mathbf{u}^{n-1} + \frac{5}{12} \mathbf{u}^{n-2}, \mathbf{u}^{n+1} \right) \\ &\leq \frac{1}{12} \Delta t \|\mathbf{u}^{n+1}\|_a^2 + \frac{23}{528} \Delta t \|\mathbf{u}^n\|_a^2 + \frac{16}{528} \Delta t \|\mathbf{u}^{n-1}\|_a^2 + \frac{5}{528} \Delta t \|\mathbf{u}^{n-2}\|_a^2 \\ &\quad + \frac{23}{6} \beta_2 \Delta t \|\mathbf{u}^n\|_S^2 + \frac{8}{3} \beta_2 \Delta t \|\mathbf{u}^{n-1}\|_S^2 + \frac{5}{6} \beta_2 \Delta t \|\mathbf{u}^{n-2}\|_S^2. \end{aligned}$$

Proof Set $\beta_1 = \frac{1}{88}$ in Lemma 2. Then $\beta_2 = 10648 C_S^2 C_{ct}^4 C_{tr}^8 C_a^{-1}$ and

$$\begin{aligned} &-2\Delta t \tilde{a}_\Gamma \left(\frac{23}{12} \mathbf{u}^n - \frac{4}{3} \mathbf{u}^{n-1} + \frac{5}{12} \mathbf{u}^{n-2}, \mathbf{u}^{n+1} \right) \\ &\leq \frac{23}{6} \Delta t \left(\beta_2 \|\mathbf{u}^n\|_S^2 + \frac{1}{88} \|\mathbf{u}^n\|_a^2 + \frac{1}{88} \|\nabla \mathbf{u}^{n+1}\|_a^2 \right) \\ &\quad + \frac{8}{3} \Delta t \left(\beta_2 \|\mathbf{u}^{n-1}\|_S^2 + \frac{1}{88} \|\nabla \mathbf{u}^{n-1}\|_a^2 + \frac{1}{88} \|\nabla \mathbf{u}^{n+1}\|_a^2 \right) \\ &\quad + \frac{5}{6} \Delta t \left(\beta_2 \|\mathbf{u}^{n-2}\|_S^2 + \frac{1}{88} \|\nabla \mathbf{u}^{n-2}\|_a^2 + \frac{1}{88} \|\nabla \mathbf{u}^{n+1}\|_a^2 \right) \\ &\leq \frac{1}{12} \Delta t \|\mathbf{u}^{n+1}\|_a^2 + \frac{23}{528} \Delta t \|\mathbf{u}^n\|_a^2 + \frac{16}{528} \Delta t \|\mathbf{u}^{n-1}\|_a^2 + \frac{5}{528} \Delta t \|\mathbf{u}^{n-2}\|_a^2 \\ &\quad + \frac{23}{6} \beta_2 \Delta t \|\mathbf{u}^n\|_S^2 + \frac{8}{3} \beta_2 \Delta t \|\mathbf{u}^{n-1}\|_S^2 + \frac{5}{6} \beta_2 \Delta t \|\mathbf{u}^{n-2}\|_S^2 \end{aligned} \quad (17)$$

99 so that the lemma is proved.

Lemma 4 *The interface term $-a_\Gamma(D_{AB}\underline{\mathbf{u}}, \underline{\mathbf{u}}) + a_{st}(D_{AB}\underline{\mathbf{u}} - D_{AM}\underline{\mathbf{u}}, \underline{\mathbf{u}})$ can be bounded by*

$$\begin{aligned}
& -2\Delta t a_\Gamma \left(\frac{23}{12}\underline{\mathbf{u}}^n - \frac{4}{3}\underline{\mathbf{u}}^{n-1} + \frac{5}{12}\underline{\mathbf{u}}^{n-2}, \underline{\mathbf{u}}^{n+1} \right) \\
& + 2\Delta t a_{st} \left(-\frac{2}{3}\underline{\mathbf{u}}^{n+1} + \frac{23}{12}\underline{\mathbf{u}}^n - \frac{7}{4}\underline{\mathbf{u}}^{n-1} + \frac{5}{12}\underline{\mathbf{u}}^{n-2} + \frac{1}{12}\underline{\mathbf{u}}^{n-3}, \underline{\mathbf{u}}^{n+1} \right) \\
& \leq \frac{58\Delta t}{360} \|\underline{\mathbf{u}}^{n+1}\|_a^2 + \frac{27\Delta t}{360} \|\underline{\mathbf{u}}^n\|_a^2 + \frac{21\Delta t}{360} \|\underline{\mathbf{u}}^{n-1}\|_a^2 + \frac{7\Delta t}{360} \|\underline{\mathbf{u}}^{n-2}\|_a^2 \\
& + \frac{\Delta t}{360} \|\underline{\mathbf{u}}^{n-3}\|_a^2 + (C_2 + 2C_3)\Delta t \|\underline{\mathbf{u}}^{n+1} - \underline{\mathbf{u}}^n\|_S^2 + 5C_3\Delta t \|\underline{\mathbf{u}}^n - \underline{\mathbf{u}}^{n-1}\|_S^2 \\
& + 2C_3\Delta t \|\underline{\mathbf{u}}^{n-1} - \underline{\mathbf{u}}^{n-2}\|_S^2 + \frac{C_3\Delta t}{3} \|\underline{\mathbf{u}}^{n-2} - \underline{\mathbf{u}}^{n-3}\|_S^2,
\end{aligned} \tag{18}$$

100 where $C_2 = 4920750C_S^2C_{ct}^4C_{tr}^8C_a^{-1}$ and $C_3 = 3375C_S^2C_{ct}^4C_{tr}^8C_a^{-1}$.

Proof Recall $a_\Gamma(\underline{\mathbf{u}}, \underline{\mathbf{u}}) = 0$. Therefore, the interface term can be rewritten as

$$\begin{aligned}
& -2\Delta t a_\Gamma \left(2\underline{\mathbf{u}}^{n+1} + \frac{23}{12}\underline{\mathbf{u}}^n - \frac{4}{3}\underline{\mathbf{u}}^{n-1} + \frac{5}{12}\underline{\mathbf{u}}^{n-2}, \underline{\mathbf{u}}^{n+1} \right) \\
& + 2\Delta t a_{st} \left(-\frac{2}{3}\underline{\mathbf{u}}^{n+1} + \frac{23}{12}\underline{\mathbf{u}}^n - \frac{7}{4}\underline{\mathbf{u}}^{n-1} + \frac{5}{12}\underline{\mathbf{u}}^{n-2} + \frac{1}{12}\underline{\mathbf{u}}^{n-3}, \underline{\mathbf{u}}^{n+1} \right) \\
& = 2\Delta t a_\Gamma (\underline{\mathbf{u}}^{n+1} - \underline{\mathbf{u}}^n, \underline{\mathbf{u}}^{n+1}) - \frac{11}{6}\Delta t a_\Gamma (\underline{\mathbf{u}}^n - \underline{\mathbf{u}}^{n-1}, \underline{\mathbf{u}}^{n+1}) \\
& + \frac{5}{6}\Delta t a_\Gamma (\underline{\mathbf{u}}^{n-1} - \underline{\mathbf{u}}^{n-2}, \underline{\mathbf{u}}^{n+1}) - \frac{4}{3}\Delta t a_{st} (\underline{\mathbf{u}}^{n+1} - \underline{\mathbf{u}}^n, \underline{\mathbf{u}}^{n+1}) \\
& + \frac{5}{2}\Delta t a_{st} (\underline{\mathbf{u}}^n - \underline{\mathbf{u}}^{n-1}, \underline{\mathbf{u}}^{n+1}) - \Delta t a_{st} (\underline{\mathbf{u}}^{n-1} - \underline{\mathbf{u}}^{n-2}, \underline{\mathbf{u}}^{n+1}) \\
& - \frac{1}{6}\Delta t a_{st} (\underline{\mathbf{u}}^{n-2} - \underline{\mathbf{u}}^{n-3}, \underline{\mathbf{u}}^{n+1}).
\end{aligned} \tag{19}$$

Similar as in the proof of Lemma 2, the first term on the right-hand side can be estimated by

$$2\Delta t a_\Gamma (\underline{\mathbf{u}}^{n+1} - \underline{\mathbf{u}}^n, \underline{\mathbf{u}}^{n+1}) \leq \frac{\Delta t}{180} \|\underline{\mathbf{u}}^{n+1}\|_a^2 + C_2\Delta t \|\underline{\mathbf{u}}^{n+1} - \underline{\mathbf{u}}^n\|_S^2 \tag{20}$$

101 and the other terms can be directly estimated by Lemma 2 with $\beta_1 = \frac{1}{60}$. The
102 desired result (18) then follows easily.

103 The following variants of the Grownwall-Bellman inequality will simplify
104 the analysis. They are particularly useful for the stability analysis of multi-step
105 methods.

Lemma 5 *Assume that $\{z_n\}$ and $\{y_n\}$ are two non-negative sequences that satisfy*

$$z_{n+1} + \xi_{-1}y_{n+1} \leq z_n + \Delta t \sum_{i=0}^k \zeta_i z_{n-i} + \sum_{i=0}^k \xi_i y_{n-i} + \Delta t \bar{z}, \tag{21}$$

where \bar{z} , ξ_i , and ζ_i are nonnegative constants and

$$\xi_{-1} \geq \sum_{i=0}^k \xi_i. \quad (22)$$

Let

$$E_n = z_n + \frac{\Delta t}{1 + \Delta t \sum_{i=0}^k \zeta_i} \sum_{i=1}^k \sum_{j=i}^k \zeta_j z_{n-i} + \frac{1}{1 + \Delta t \sum_{i=0}^k \zeta_i} \sum_{i=0}^k \sum_{j=i}^k \xi_j y_{n-i}. \quad (23)$$

Then

$$E_n \leq e^{\sum_{i=0}^k \zeta_i t} \left(E_k + \frac{\bar{z}}{\sum_{i=0}^k \zeta_i} \right) \quad (24)$$

106 for any $n\Delta t \leq t$.

Proof From the definition of E_n and the constraint (22), we have

$$E_{n+1} \leq (1 + \Delta t \sum_{i=0}^k \zeta_i) E_n + \Delta t \bar{z} \quad (25)$$

107 so that the bound (24) is easily derived via recursion.

108 Another variant of Grownwall-Bellman inequality will be useful in the long
109 time stability analysis.

Lemma 6 Assume that $\{z_n\}$ and $\{y_n\}$ are two nonnegative sequences that satisfy

$$z_{n+1} + \zeta_{-1} \Delta t y_{n+1} \leq z_n + \Delta t \sum_{i=0}^k \zeta_i y_{n-i} + \Delta t \bar{z}, \quad (26)$$

where ζ_i , $i = -1, \dots, k$, are nonnegative constants and

$$\bar{\zeta} = \frac{1}{k+1} \left(\zeta_{-1} - \sum_{i=0}^k \zeta_i \right) > 0. \quad (27)$$

Let

$$E_n = z_n + \Delta t \sum_{i=0}^k \left((k-i)\bar{\zeta} + \sum_{j=i}^k \zeta_j \right) y_{n-i}. \quad (28)$$

Then

$$E_{n+1} + \bar{\zeta} \Delta t \sum_{i=0}^k y_{n+1-i} \leq E_n + \Delta t \bar{z}. \quad (29)$$

Moreover, if $z_{n+1} \leq C_\zeta y_{n+1}$, then

$$E_n \leq (1 + \bar{C} \Delta t)^{-(n-k)} E_k + \frac{\bar{z}}{\bar{C}}, \quad (30)$$

where

$$\bar{C} = \min \left\{ \frac{\bar{\zeta}}{2C_\zeta}, \frac{\bar{\zeta}}{2(\zeta_{-1} - \bar{\zeta})\Delta t} \right\}. \quad (31)$$

110 *Proof* Let $d_i = (k-i)\bar{\zeta} + \sum_{j=i}^k \zeta_j$. Then $E_n = z_n + \Delta t \sum_{i=0}^k d_i y_{n-i}$. It is easily
111 verified that

$$d_0 + \bar{\zeta} = \zeta_{-1}, \quad (32)$$

$$d_i - d_{i+1} - \bar{\zeta} = \zeta_i, \quad \text{for } i = 1, \dots, k-1, \quad (33)$$

$$d_k = \zeta_k, \quad (34)$$

so the inequality (26) can be recast as

$$z_{n+1} + \Delta t(d_0 + \bar{\zeta})y_{n+1} \leq z_n + \Delta t \sum_{i=0}^{k-1} (d_i - d_{i+1} - \bar{\zeta})y_{n-i} + \Delta t d_k y_{n-k} + \Delta t \bar{z} \quad (35)$$

or

$$z_{n+1} + \Delta t \sum_{i=0}^k d_i y_{n+1-i} + \bar{\zeta} \Delta t \sum_{i=0}^k y_{n+1-i} \leq z_n + \Delta t \sum_{i=0}^k d_i y_{n-i} + \Delta t \bar{z}, \quad (36)$$

112 which is exactly the inequality (29). Now, if $z_{n+1} \leq C_\zeta y_{n+1}$, then

$$\begin{aligned} \sum_{i=0}^k y_{n+1-i} &\geq \frac{1}{2C_\zeta} z_{n+1} + \frac{y_{n+1}}{2} + \sum_{i=1}^k y_{n+1-i} \\ &\geq \frac{1}{2C_\zeta} z_{n+1} + \Delta t \tilde{C} \sum_{i=0}^k d_i y_{n+1-i}, \end{aligned} \quad (37)$$

where $\tilde{C} = \frac{1}{\Delta t} \min\{\frac{1}{2d_0}, \min\{d_i^{-1}\}_{i=1}^k\} = \frac{1}{2d_0 \Delta t}$. Note that $d_0 = k\bar{\zeta} + \sum_{j=0}^k \zeta_j = \zeta_{-1} - \bar{\zeta}$ so that

$$\bar{\zeta} \sum_{i=0}^k y_{n+1-i} \geq \bar{C} (z_{n+1} + \Delta t \sum_{i=0}^k d_i y_{n+1-i}) = \bar{C} E_{n+1}, \quad (38)$$

where \bar{C} is defined in (31). Then, from (29), we have

$$(1 + \bar{C} \Delta t) E_{n+1} \leq E_n + \Delta t \bar{z}. \quad (39)$$

113 Now by recursion, we have

$$\begin{aligned} E_n &\leq (1 + \bar{C} \Delta t)^{-(n-k)} E_k + \Delta t \bar{z} \sum_{i=1}^{n-k} (1 + \bar{C} \Delta t)^{-i} \\ &\leq (1 + \bar{C} \Delta t)^{-(n-k)} E_k + \frac{\bar{z}}{\bar{C}} \end{aligned} \quad (40)$$

114 so that the lemma is proved.

115 Additional sequences are considered in the following lemma.

Lemma 7 Assume that $\{z_n\}$ and $\{y_n^\ell\}$, $\ell = 1, \dots, L$, are nonnegative sequences that satisfy

$$z_{n+1} + \Delta t \sum_{\ell=1}^L \zeta_{-1}^\ell y_{n+1}^\ell \leq z_n + \Delta t \sum_{\ell=1}^L \sum_{i=0}^{k_\ell} \zeta_i^\ell y_{n-i}^\ell + \Delta t \bar{z}, \quad (41)$$

where ζ_i^ℓ , $\ell = 1, \dots, L$ and $i = -1, \dots, k_\ell$, are nonnegative constants with $1 \leq k_\ell \leq k$, and

$$\bar{\zeta}^\ell = \frac{1}{k_\ell + 1} \left(\zeta_{-1}^\ell - \sum_{i=0}^{k_\ell} \zeta_i^\ell \right) > 0. \quad (42)$$

Define

$$E_n = z_n + \Delta t \sum_{\ell=1}^L \sum_{i=0}^{k_\ell} \left((k_\ell - i) \bar{\zeta}^\ell + \sum_{j=i}^{k_\ell} \zeta_j^\ell \right) y_{n-i}^\ell. \quad (43)$$

Then

$$E_{n+1} + \Delta t \sum_{\ell=1}^L \bar{\zeta}^\ell \sum_{i=0}^{k_\ell} y_{n+1-i}^\ell \leq E_n + \Delta t \bar{z}. \quad (44)$$

In addition, assume that $z_{n+1} \leq C_\zeta y_{n+1}^{\ell_0}$ for some ℓ_0 . Then

$$E_n \leq (1 + \bar{C} \Delta t)^{-(n-k)} E_k + \frac{\bar{z}}{\bar{C}}, \quad (45)$$

where

$$\bar{C} = \min \left\{ \frac{\bar{\zeta}^{\ell_0}}{2C_\zeta}, \min_{\ell} \frac{\bar{\zeta}^\ell}{2(\zeta_{-1}^\ell - \bar{\zeta}^\ell) \Delta t} \right\}. \quad (46)$$

116 The proof is very much the same as that for Lemma 6 and thus is omitted
117 here.

118 *Unconditional stability.* Now we can prove that our novel AMB3 scheme is
119 unconditionally stable over any finite time.

120 **Theorem 1** Let $T > 0$ be any fixed time. Then, the AMB3 scheme (9) is
121 unconditionally stable in $(0, T]$.

Proof Set $\underline{\mathbf{v}} = 2\Delta t \underline{\mathbf{u}}^{n+1}$ in (9). Using of $\langle 2a, a - b \rangle = |a|^2 + |a - b|^2 - |b|^2$, we obtain

$$\begin{aligned} & \|\underline{\mathbf{u}}^{n+1}\|_S^2 - \|\underline{\mathbf{u}}^n\|_S^2 + \|\underline{\mathbf{u}}^{n+1} - \underline{\mathbf{u}}^n\|^2 + 2\Delta t \tilde{a} (D_{AM} \underline{\mathbf{u}}^{n+1}, \underline{\mathbf{u}}^{n+1}) \\ & = 2\Delta t \langle D_{AM} \underline{\mathbf{f}}^{n+1}, \underline{\mathbf{u}}^{n+1} \rangle - 2\Delta t \tilde{a}_\Gamma (D_{AB} \underline{\mathbf{u}}^{n+1}, \underline{\mathbf{u}}^{n+1}), \end{aligned} \quad (47)$$

where the pressure term $b(\underline{\mathbf{u}}^{n+1}, \frac{2}{3}p^{n+1} + \frac{5}{12}p^{n-1} - \frac{1}{12}p^{n-3}) = 0$ because $\underline{\mathbf{u}}^{n+1} \in \mathbf{H}_f$ and $p^{n+1}, p^{n-1}, p^{n-3} \in \mathbf{Q}$. A crucial observation is that the last term on

the left-hand-side can be bounded below, i.e., according to Young's inequality, we have

$$\begin{aligned}
& 2\tilde{a} \left(\frac{2}{3} \underline{\mathbf{u}}^{n+1} + \frac{5}{12} \underline{\mathbf{u}}^{n-1} - \frac{1}{12} \underline{\mathbf{u}}^{n-3}, \underline{\mathbf{u}}^{n+1} \right) \\
& \geq 2 \left(\frac{2}{3} \|\underline{\mathbf{u}}^{n+1}\|_{\tilde{a}}^2 - \frac{5}{24} (\|\underline{\mathbf{u}}^{n-1}\|_{\tilde{a}}^2 + \|\underline{\mathbf{u}}^{n+1}\|_{\tilde{a}}^2) - \frac{1}{24} (\|\underline{\mathbf{u}}^{n-3}\|_{\tilde{a}}^2 + \|\underline{\mathbf{u}}^{n+1}\|_{\tilde{a}}^2) \right) \\
& \geq \frac{5}{6} \|\underline{\mathbf{u}}^{n+1}\|_{\tilde{a}}^2 - \frac{5}{12} \Delta t \|\underline{\mathbf{u}}^{n-1}\|_{\tilde{a}}^2 - \frac{1}{12} \Delta t \|\underline{\mathbf{u}}^{n-3}\|_{\tilde{a}}^2.
\end{aligned} \tag{48}$$

122 This implies that the special Adams-Moulton operator that we developed is
123 dissipative because the coefficient of the positive term is larger than the sum
124 of the coefficients of the negative terms. This fact will be exploited heavily
125 below to prove the unconditional stability as well as the long-time stability of
126 the scheme.

We also notice that the forcing term on the right-hand-side can be bounded above according to Young's inequality:

$$\begin{aligned}
2 \langle D_{AM} \underline{\mathbf{f}}^{n+1}, \underline{\mathbf{u}}^{n+1} \rangle & \leq \frac{1}{6C_P^2} C_a \|\underline{\mathbf{u}}^{n+1}\|^2 + 6C_P^2 C_a^{-1} \|D_{AM} \underline{\mathbf{f}}^{n+1}\|^2 \\
& \leq \frac{1}{6} \|\underline{\mathbf{u}}^{n+1}\|_{\tilde{a}}^2 + \beta_3 \max_i \|\underline{\mathbf{f}}^i\|^2,
\end{aligned} \tag{49}$$

where $\beta_3 = 10C_P^2 C_a^{-1}$. Combining the above estimates with Lemma 3 and discarding the term $\|\underline{\mathbf{u}}^{n+1} - \underline{\mathbf{u}}^n\|_S^2$, we have

$$\begin{aligned}
& \|\underline{\mathbf{u}}^{n+1}\|_S^2 + \frac{308}{528} \Delta t \|\underline{\mathbf{u}}^{n+1}\|_{\tilde{a}}^2 \\
& \leq (1 + \frac{23}{6} \beta_2 \Delta t) \|\underline{\mathbf{u}}^n\|_S^2 + \frac{8}{3} \beta_2 \Delta t \|\underline{\mathbf{u}}^{n-1}\|_S^2 + \frac{5}{6} \beta_2 \Delta t \|\underline{\mathbf{u}}^{n-2}\|_S^2 + \frac{23}{528} \Delta t \|\underline{\mathbf{u}}^n\|_{\tilde{a}}^2 \\
& \quad + \frac{236}{528} \Delta t \|\underline{\mathbf{u}}^{n-1}\|_{\tilde{a}}^2 + \frac{5}{528} \Delta t \|\underline{\mathbf{u}}^{n-2}\|_{\tilde{a}}^2 + \frac{44}{528} \Delta t \|\underline{\mathbf{u}}^{n-3}\|_{\tilde{a}}^2 + \beta_3 \Delta t \max_i \|\underline{\mathbf{f}}^i\|^2.
\end{aligned}$$

Now, define

$$\begin{aligned}
E_n & = \|\underline{\mathbf{u}}^n\|_S^2 + \frac{7\beta_2 \Delta t}{2(1 + \frac{22}{3} \beta_2 \Delta t)} \|\underline{\mathbf{u}}^{n-1}\|_S^2 + \frac{5\beta_2 \Delta t}{6(1 + \frac{22}{3} \beta_2 \Delta t)} \|\underline{\mathbf{u}}^{n-2}\|_S^2 \\
& \quad + \frac{308 \Delta t}{528(1 + \frac{22}{3} \beta_2 \Delta t)} \|\underline{\mathbf{u}}^n\|_{\tilde{a}}^2 + \frac{285 \Delta t}{528(1 + \frac{22}{3} \beta_2 \Delta t)} \|\underline{\mathbf{u}}^{n-1}\|_{\tilde{a}}^2 \\
& \quad + \frac{49 \Delta t}{528(1 + \frac{22}{3} \beta_2 \Delta t)} \|\underline{\mathbf{u}}^{n-2}\|_{\tilde{a}}^2 + \frac{44 \Delta t}{528(1 + \frac{22}{3} \beta_2 \Delta t)} \|\underline{\mathbf{u}}^{n-3}\|_{\tilde{a}}^2.
\end{aligned} \tag{50}$$

We then have, by Lemma 5

$$\|\underline{\mathbf{u}}^{n+1}\|_S^2 \leq E_n \leq e^{\frac{22}{3} \beta_2 T} \left(E_3 + \frac{3\beta_3}{22\beta_2} \max_i \|\underline{\mathbf{f}}^i\|^2 \right), \tag{51}$$

127 on any finite time interval $[0, T]$.

128 *Long-time stability.* We next show that our scheme is long-time stable in the
 129 sense that the solutions will remain bounded uniformly in time as long as
 130 a time-step restriction is satisfied. As a direct consequence of this long-time
 131 stability, we are able to show that we are able to derive uniform in time bounds
 132 on the error.

Theorem 2 *Assume that $\mathbf{f} \in L^\infty(L^2(\Omega))$. For the AMB3 scheme, there exists $\Delta t_0 > 0$ such that the solution is uniformly bounded in time if $\Delta t \leq \Delta t_0$. In particular, there exist $0 < \lambda_1 < 1, 0 < \lambda_2 < \infty$, and $E_3 \geq 0$ such that*

$$\|\underline{\mathbf{u}}^{n+1}\|^2 \leq \lambda_1^{n-2} E_3 + \lambda_2.$$

Proof After rearranging (47) in a slightly different way, we have

$$\begin{aligned} & \|\underline{\mathbf{u}}^{n+1}\|_S^2 - \|\underline{\mathbf{u}}^n\|_S^2 + \|\underline{\mathbf{u}}^{n+1} - \underline{\mathbf{u}}^n\|_S^2 + 2\Delta t a (D_{AM}\underline{\mathbf{u}}^{n+1}, \underline{\mathbf{u}}^{n+1}) \\ &= 2\Delta t \langle D_{AM}\underline{\mathbf{f}}^{n+1}, \underline{\mathbf{u}}^{n+1} \rangle - 2\Delta t a_\Gamma (D_{AB}\underline{\mathbf{u}}^{n+1}, \underline{\mathbf{u}}^{n+1}) \\ & \quad + 2\Delta t a_{st} (D_{AB}\underline{\mathbf{u}}^{n+1} - D_{AM}\underline{\mathbf{u}}^{n+1}, \underline{\mathbf{u}}^{n+1}). \end{aligned} \quad (52)$$

Similar to the proof of the previous theorem, the bilinear term on the left-hand-side can be bounded from below by

$$2a (D_{AM}\underline{\mathbf{u}}^{n+1}, \underline{\mathbf{u}}^{n+1}) \geq \frac{5}{6} \|\underline{\mathbf{u}}^{n+1}\|_a^2 - \frac{5}{12} \|\underline{\mathbf{u}}^{n-1}\|_a^2 - \frac{1}{12} \|\underline{\mathbf{u}}^{n-3}\|_a^2 \quad (53)$$

and the forcing term can be bounded from above by

$$2 \langle D_{AM}\underline{\mathbf{f}}^{n+1}, \underline{\mathbf{u}}^{n+1} \rangle \leq \frac{1}{180} \|\underline{\mathbf{u}}^{n+1}\|_a^2 + \beta_4 \max_i \|\underline{\mathbf{f}}^i\|^2, \quad (54)$$

where $\beta_4 = 300C_P^2C_a^{-1}$. The interface term has been estimated in Lemma 4. Combine the above inequalities with Lemma 4, we have

$$\begin{aligned} & \|\underline{\mathbf{u}}^{n+1}\|_S^2 + \frac{240}{360} \Delta t \|\underline{\mathbf{u}}^{n+1}\|_a^2 + [1 - (C_2 + 2C_3)\Delta t] \|\underline{\mathbf{u}}^{n+1} - \underline{\mathbf{u}}^n\|_S^2 \\ & \leq \|\underline{\mathbf{u}}^n\|_S^2 + \frac{27}{360} \Delta t \|\underline{\mathbf{u}}^n\|_a^2 + \frac{171}{360} \Delta t \|\underline{\mathbf{u}}^{n-1}\|_a^2 + \frac{7}{360} \Delta t \|\underline{\mathbf{u}}^{n-2}\|_a^2 \\ & \quad + \frac{31}{360} \Delta t \|\underline{\mathbf{u}}^{n-3}\|_a^2 + 5C_3 \Delta t \|\underline{\mathbf{u}}^n - \underline{\mathbf{u}}^{n-1}\|_S^2 + 2C_3 \Delta t \|\underline{\mathbf{u}}^{n-1} - \underline{\mathbf{u}}^{n-2}\|_S^2 \\ & \quad + \frac{C_3 \Delta t}{3} \|\underline{\mathbf{u}}^{n-2} - \underline{\mathbf{u}}^{n-3}\|_S^2 + \beta_4 \Delta t \max_i \|\underline{\mathbf{f}}^i\|^2. \end{aligned} \quad (55)$$

We require that

$$1 - (C_2 + 2C_3)\Delta t > \frac{22C_3}{3} \Delta t. \quad (56)$$

A convenient choice is

$$\Delta t_0 \leq \frac{1}{C_2 + \frac{31}{3}C_3} \quad (57)$$

such that $1 - (C_2 + 2C_3)\Delta t \geq \frac{25C_3}{3}\Delta t$ if $\Delta t \leq \Delta t_0$. Let

$$\begin{aligned} E_n &= \|\underline{\mathbf{u}}^n\|_S^2 + \frac{239}{360}\Delta t\|\underline{\mathbf{u}}^n\|_a^2 + \frac{211}{360}\Delta t\|\underline{\mathbf{u}}^{n-1}\|_a^2 + \frac{39}{360}\Delta t\|\underline{\mathbf{u}}^{n-2}\|_a^2 \\ &+ \frac{31}{360}\Delta t\|\underline{\mathbf{u}}^{n-3}\|_a^2 + \frac{24C_3\Delta t}{3}\|\underline{\mathbf{u}}^n - \underline{\mathbf{u}}^{n-1}\|_S^2 \\ &+ \frac{8C_3\Delta t}{3}\|\underline{\mathbf{u}}^{n-1} - \underline{\mathbf{u}}^{n-2}\|_S^2 + \frac{C_3\Delta t}{3}\|\underline{\mathbf{u}}^{n-2} - \underline{\mathbf{u}}^{n-3}\|_S^2. \end{aligned} \quad (58)$$

Note that $\|\underline{\mathbf{u}}^{n+1}\|_S^2 \leq C_\zeta\|\underline{\mathbf{u}}^{n+1}\|_a^2$, where $C_\zeta = C_P^2 C_a^{-2} C_s^{-2}$. By Corollary 7, we arrive at the conclusion

$$\|\underline{\mathbf{u}}^{n+1}\|_S^2 \leq E_{n+1} \leq (1 + \bar{C}\Delta t)^{n-2} E_3 + \bar{C}^{-1}\beta_4 \max_i \|\mathbf{f}\|^2, \quad (59)$$

133 where $\bar{C} = \min\{\frac{1}{720C_\zeta}, \frac{1}{478}\}$. The theorem is proven if we set $\lambda_1 = (1 + \bar{C}\Delta t)^{-1}$
134 and $\lambda_2 = \bar{C}^{-1}\beta_4 \max_i \|\mathbf{f}\|^2$.

135 An immediate consequence of the previous theorem is the following uniform
136 in time error bound. This is a highly desirable property because the retention
137 and release of contaminants in karst aquifers usually occur over very long time
138 scales.

Theorem 3 *Suppose that the solutions $\underline{\mathbf{u}}$ and p are smooth and bounded uniformly in time. Let $\underline{\mathbf{e}}^n := \underline{\mathbf{u}}(n\Delta t) - \underline{\mathbf{u}}^n$ denote the error. Then, provided that the time-step restriction as in the previous theorem is satisfied, we have the estimates*

$$\|\underline{\mathbf{e}}^{n+1}\|^2 \leq (1 + \bar{C}\Delta t)^{-n+2} \epsilon_3^2 + C_4(\Delta t)^6,$$

where \bar{C} and C_4 are appropriate positive constants, and

$$\begin{aligned} \epsilon_3^2 &= \|\underline{\mathbf{e}}^3\|_S^2 + \frac{239}{360}\Delta t\|\underline{\mathbf{e}}^3\|_a^2 + \frac{211}{360}\Delta t\|\underline{\mathbf{e}}^2\|_a^2 + \frac{39}{360}\Delta t\|\underline{\mathbf{e}}^1\|_a^2 \\ &+ \frac{24C_3\Delta t}{3}\|\underline{\mathbf{e}}^3 - \underline{\mathbf{e}}^2\|_S^2 + \frac{8C_3\Delta t}{3}\|\underline{\mathbf{e}}^2 - \underline{\mathbf{e}}^1\|_S^2 + \frac{C_3\Delta t}{3}\|\underline{\mathbf{e}}^1\|_S^2. \end{aligned}$$

Proof Because $\underline{\mathbf{u}}, p$ are smooth and bounded, and since the scheme 9 is third-order in time, we have that the solution satisfies the scheme in the form of

$$\begin{aligned} &\left\langle \left\langle \frac{\underline{\mathbf{u}}((n+1)\Delta t) - \underline{\mathbf{u}}(n\Delta t)}{\Delta t}, \underline{\mathbf{v}} \right\rangle \right\rangle + \tilde{a}(D_{AM}\underline{\mathbf{u}}((n+1)\Delta t), \underline{\mathbf{v}}) \\ &+ b(\underline{\mathbf{v}}, D_{AMP}((n+1)\Delta t)) = \langle D_{AM}\underline{\mathbf{f}}^{n+1}, \underline{\mathbf{v}} \rangle - \tilde{a}_\Gamma(D_{AB}\underline{\mathbf{u}}((n+1)\Delta t), \underline{\mathbf{v}}) \\ &+ (R^{n+1}, \underline{\mathbf{v}}), \\ &b(D_{AM}\underline{\mathbf{u}}((n+1)\Delta t), q) = 0, \end{aligned}$$

where the remainder term R^n is uniformly bounded by

$$\|R^n\| \leq C(\Delta t)^3 \quad \forall n = 1, 2, \dots$$

This implies that the error \mathbf{e}^n satisfies

$$\begin{aligned} \left\langle \left\langle \frac{\mathbf{e}^{n+1} - \mathbf{e}^n}{\Delta t}, \mathbf{v} \right\rangle \right\rangle + \tilde{a}(D_{AM}\mathbf{e}^{n+1}, \mathbf{v}) + b(\mathbf{v}, D_{AM}e_p^{n+1}) \\ = -\tilde{a}_\Gamma(D_{AB}\mathbf{e}^{n+1}, \mathbf{v}) + (R^{n+1}, \mathbf{v}), \\ b(D_{AM}\mathbf{e}^{n+1}, q) = 0, \end{aligned}$$

139 where $e_p^n = p(n\Delta t) - p^n$. Repeating the same argument as in the previous
140 theorem leads to the desired estimate. Therefore, we have a third-order uniform
141 in time error bound provided that the time-step restriction is satisfied and that
142 the scheme is initiated properly so that ϵ_3 is of third-order. This ends the proof
143 of uniform in time third-order error bound.

144 **Remark 4** *If a conforming finite element is used, the scheme is still long-*
145 *time stable under the constraint $\Delta t \leq \Delta t_0$ where Δt_0 is independent of the*
146 *finite element mesh size h . Moreover, based on the stability analysis, we can*
147 *prove that the AMB3 scheme is third-order temporal accurate. Following the*
148 *analysis in [16], if the Taylor-Hood (P2-P1) finite element pair is used for the*
149 *discretization of the Stokes system and continuous piecewise quadratic (P2)*
150 *finite elements are used for discretization of the Darcy system, the error of the*
151 *fully discretized scheme will be $\|\mathbf{u}^n(t) - \mathbf{u}_h^n\| = O(\Delta t^3 + h^3)$, which is illustrated*
152 *by the numerical results in next section.*

153 4 Numerical results

154 We report here on the results of several numerical experiments. The numerical
155 results illustrate the third-order accuracy, unconditional stability, and the long-
156 time stability and uniform in time error bounds.

Suppose that the error behaves like $O(h^{\theta_1} + \Delta t^{\theta_2})$. Then, if we set $\Delta t = h^\theta$, the rate of convergence would be of the order of $r_{h,\theta} = \min(\theta_1, \theta\theta_2)$ with respect to h . The rate of convergence can be numerically estimated by calculating

$$r_{h,\theta} \approx \log_2 \frac{\|u_{2h,\theta} - u_{exact}\|_{l^2}}{\|u_{h,\theta} - u_{exact}\|_{l^2}}. \quad (60)$$

157 Here, we use the discrete l^2 norm of nodal values to measure errors.

158 We set $\Omega_f = (0, 1) \times (1, 2)$, $\Omega_p = (0, 1) \times (0, 1)$, and the interface $\Gamma = (0, 1) \times$
159 $\{1\}$ which separates Ω_f and Ω_p . Uniform triangular meshes are created by first
160 dividing the rectangular domains Ω_p and Ω_f into identical small squares and
161 then dividing each square into two triangles. With respect to such grids, the
162 Taylor-Hood (P2-P1) finite element pair is used to discretize the Stokes system
163 so that the conduit fluid velocity \mathbf{u}_h is approximated by continuous piecewise
164 quadratic functions and the conduit pressure p is approximated by continuous
165 piecewise linear functions. Continuous piecewise quadratic functions are used
166 to approximate the hydraulic head ϕ_h .

167 4.1 Convergence rates

We choose the manufactured solution of the Stokes-Darcy system (1) given by

$$\begin{aligned}\mathbf{u}_f(\mathbf{x}, t) &= \left(-\frac{1}{\pi}e^y \sin \pi x \cos 2\pi t, (e^y - e) \cos \pi x \cos 2\pi t \right), \\ p_f(\mathbf{x}, t) &= 2e^y \cos \pi x \cos 2\pi t, \\ \phi(\mathbf{x}, t) &= (e^y - ey) \cos \pi x \cos 2\pi t.\end{aligned}$$

168 The right-hand side data in the partial differential equations, initial conditions,
169 and boundary conditions are then chosen correspondingly. Here, we set $\Delta t = h$,
170 $\mathbb{K} = \mathbb{I}$, $\nu = g = S = \gamma_f = \gamma_p = 1$, $T = 1$, and $\alpha_{BJSJ} = 1$.

171 Table 1 shows that the numerical convergence rate is approximately third
172 order for ϕ and \mathbf{u} , and of a bit over second order for p . This is all consistent with
173 the third-order temporal scheme and the Taylor-Hood (P2-P1) finite element
174 pair for the Stokes equations and the the P2 element for the Darcy equation.

h	e_ϕ	e_u	e_p
1/16	1.40e-3	6.49e-4	1.35e-2
1/32	2.05e-4	9.44e-5	1.97e-3
1/64	2.70e-5	1.24e-5	3.36e-4
1/128	3.45e-6	1.58e-6	6.55e-5
1/256	4.36e-7	1.99e-7	1.41e-5
1/512	5.45e-8	2.49e-8	3.26e-6
$r_{terminal}$	3.00	3.00	2.11

Table 1 Relative error and order of accuracy with respect to the spatial grid size h for Example 4.1 at $t = 1$ and with $\Delta t = h$ and $r_{terminal} = r_{1/512,1}$ defined by (60).

175 4.2 Long-time error

To illustrate the long-time behavior of our schemes, we use the following manufactured solution that is a slight modification of one used in [9]:

$$\begin{aligned}\mathbf{u}_f(\mathbf{x}, t) &= \left([x^2y^2 + e^{-y}], [-\frac{2}{3}xy^3 + [2 - \pi \sin(\pi x)]] \right) [2 + \cos(2\pi t)] \\ p_f(\mathbf{x}, t) &= -[2 - \pi \sin(\pi x)] \cos(2\pi y) [2 + \cos(2\pi t)] \\ \phi(\mathbf{x}, t) &= [2 - \pi \sin(\pi x)] [-y + \cos(\pi(1 - y))] [2 + \cos(2\pi t)].\end{aligned}$$

176 The right-hand side data in the partial differential equations, initial conditions,
177 and boundary conditions are then chosen correspondingly. Here, we set $\mathbb{K} = \mathbb{I}$,
178 $\nu = g = S = 1$, $T = 1$, and $\alpha_{BJSJ} = 1$. In this long time numerical experiment,
179 we set the terminal time $T = 100$ and $h = 1/64$. Figure 2 displays the relative
180 error as a function of t for two different values of Δt . We see that the long-time
181 error remains bounded, and indeed, seems to not grow.

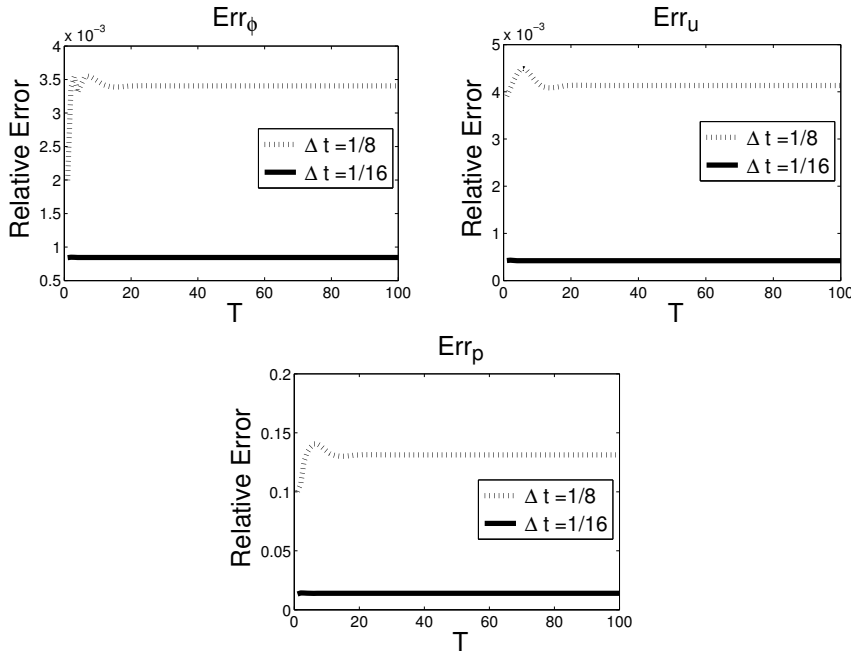


Fig. 2 Relative error for the hydraulic head in the matrix ϕ (top-left), conduit velocity \mathbf{u} (top-right), and conduit pressure p (bottom) for $0 \leq t \leq 100$ for $h = 1/64$.

182 4.3 Long-time stability analysis

We use the same domain and the same initial conditions as in the Section 4.2, i.e., we have

$$\begin{aligned} \mathbf{u}_f(\mathbf{x}, 0) &= \left(-\frac{1}{\pi} e^y \sin \pi x, (e^y - e) \cos \pi x \right), \\ p_f(\mathbf{x}, 0) &= 2e^y \cos \pi x, \\ \phi(\mathbf{x}, 0) &= (e^y - ey) \cos \pi x, \end{aligned}$$

183 but now the forcing terms are set to zero and homogeneous Dirichlet boundary
 184 conditions are imposed on the hydraulic head ϕ and conduit flow velocity
 185 \mathbf{u} . To study the long-time stability of the scheme, we define the functionals
 186 $E_\phi = \|\phi\|_{l^2}^2$, $E_{\mathbf{u}} = \|\mathbf{u}\|_{l^2}^2$, and $E_p = \|p\|_{l^2}^2$. The final time is set to $T = 100$.

187 For Figure 3, we set $h = 1/128$, $\Delta t = 1/10$, $\mathbb{K} = \mathbb{I}$, $\nu = g = S = 1$, and
 188 $\gamma_f = \gamma_p = 0$. The energy does decay as time evolves, which suggests that the
 189 long-time stability time-step size constraint in the analysis is satisfied with the
 190 above choices for the parameters.

191 For Figure 4, we set $h = 1/128$, $\mathbb{K} = \mathbb{I}$, $\nu = 0.0001$, $g = S = 1$, and
 192 $\gamma_f = \gamma_p = 0$. The figure shows that for this choice of ν , the time-step constraint
 193 is between $1/15$ and $1/10$ which is more restrictive compared to that for Figure
 194 3 for which $\nu = 1$. Thus, we note that the theoretical time step size constraint

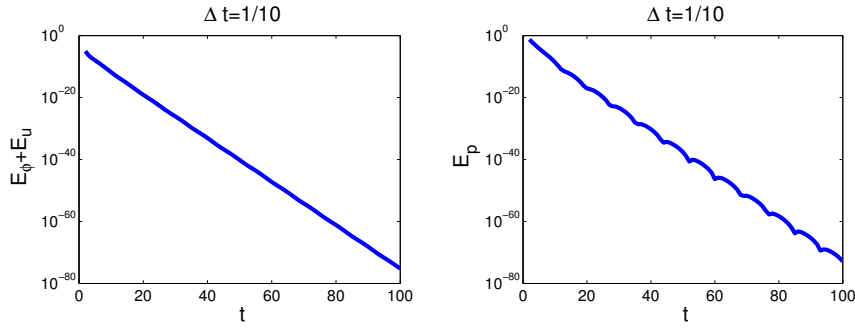


Fig. 3 Long-time behavior of the functionals $E_\phi + E_{\mathbf{u}}$ (left) and E_p (right) for $\nu = 1$ and $\mathbb{K} = \mathbb{I}$.

195 (57) decreases as ν becomes smaller so that the long-time numerical results of
 196 Figures 3 and 4 are consistent with our long-time stability analysis.

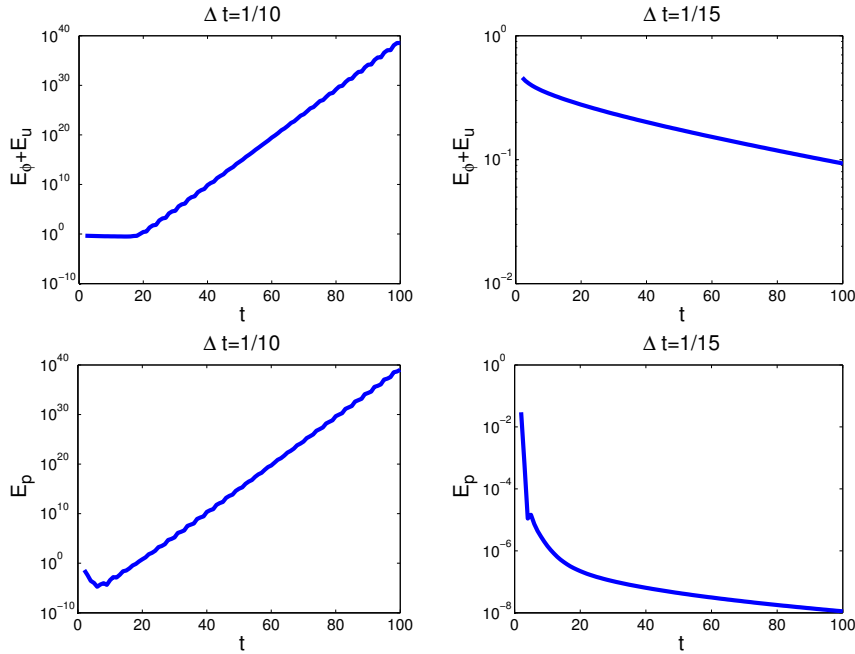


Fig. 4 Long-time behavior of the functionals $E_\phi + E_{\mathbf{u}}$ (top row) and E_p (bottom row) for $\nu = 0.0001$ and $\mathbb{K} = \mathbb{I}$.

196 For Figure 5, we set $h = 1/128$, $\mathbb{K} = 0.01\mathbb{I}$, $\nu = g = S = 1$, and $\gamma_f = \gamma_p = 0$.
 197 The figure shows that for this choice of \mathbb{K} , the time-step constraint is between
 198 $1/50$ and $1/45$ which is more restrictive compared to that for Figure 3 for
 199 $1/50$ and $1/45$ which is more restrictive compared to that for Figure 3 for
 200 which $\mathbb{K} = \mathbb{I}$. Thus, again, the long-time numerical results of Figures 3 and

201 5 are consistent with the theoretical time-step size constraint (57), i.e., the
 202 time-step constraint becomes smaller as the minimum eigenvalue of \mathbb{K} becomes
 smaller.

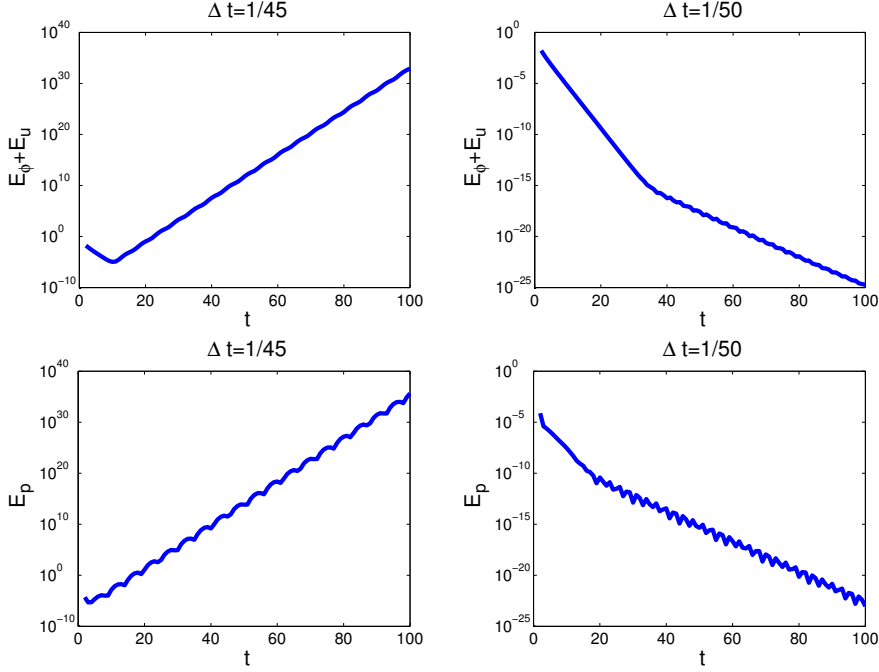


Fig. 5 Long-time behavior of the functionals $E_\phi + E_u$ (top row) and E_p (bottom row) for $\nu = 1$ and $\mathbb{K} = 0.01\mathbb{I}$.

203

204 For Figure 6, we set $h = 1/128$, $\mathbb{K} = 0.01\mathbb{I}$, $\nu = g = S = 1$, and $\gamma_f =$
 205 $\gamma_p = g/2$. The figure shows that for this choice of γ_f and γ_p , the time-step
 206 constraint is between $1/45$ and $1/40$ which is less restrictive compared to that
 207 for Figure 5 for which $\gamma_f = \gamma_p = 0$. Thus the results show that the stabilizing
 208 term does provide better long-time stability.

209 5 Concluding remarks

210 We proposed and investigated a long-time, third-order accurate, and effi-
 211 cient numerical method for coupled Stokes-Darcy systems. The algorithm is
 212 a combination of a novel third-order Adams-Moulton method and a Adams-
 213 Bashforth method. Our algorithm is a special case of the class of implicit-
 214 explicit (IMEX) schemes. The interfacial term that requires communications
 215 between the porous media and conduit, i.e., between the Stokes and Darcy
 216 components of the model, is treated explicitly in our scheme so that, at each
 217 time step, only two decoupled problems (one Stokes and one Darcy) are solved.

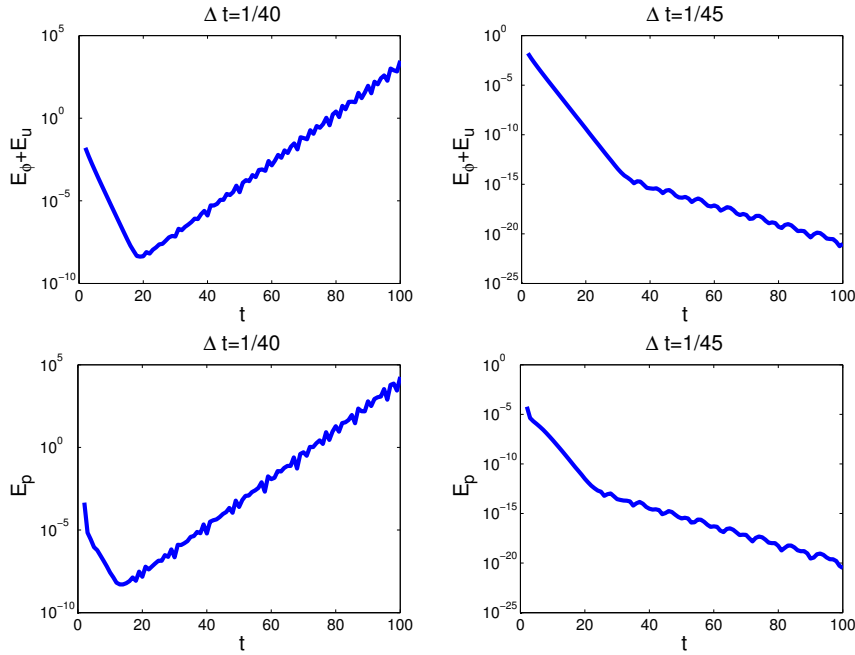


Fig. 6 Long-time behavior of the functionals $E_\phi + E_u$ (top row) and E_p (bottom row) for $\nu = 1$, $\mathbb{K} = 0.01\mathbb{I}$, and $\gamma_f = \gamma_p = g/2$.

218 Therefore, our scheme can be implemented very efficiently and, in particular,
 219 legacy codes can be used for each component.

220 We have shown that our scheme is unconditionally stable and, with a
 221 mild time-step restriction, long-time stable in the sense that solutions remain
 222 bounded uniformly in time. The uniform bound in time of the solution leads
 223 to uniform in time error estimates. This is a highly desirable feature because
 224 the physically interesting phenomena of contaminant sequestration and re-
 225 lease usually occur over a very long time scale and one would like to have
 226 faithful numerical results over such time scales. The estimates are illustrated
 227 by numerical examples. All these features suggest that the method has strong
 228 potential in real applications.

229 Methods having even higher-order temporal accuracy and the desired un-
 230 conditional and long-time stability can be derived via suitable combination of
 231 a higher-order Adams-Moulton method for the dissipative term and a stan-
 232 dard Adams-Bashforth method for the interface term. Details will be reported
 233 on elsewhere.

234 References

- 235 1. G. AKRIVIS, M. CROUZEIX, AND C. MAKRIDAKIS, *Implicit-explicit multistep finite element*
 236 *methods for nonlinear parabolic problems*, Math. Comp, 67 (1998), pp. 457-477.

- 237 2. G. AKRIVIS, M. CROUZEIX, AND C. MAKRIDAKIS, *Implicit-explicit multistep methods for*
238 *quasilinear parabolic equations*, Numer. Math., 82 (1999), pp. 521-541.
- 239 3. G. AKRIVIS AND Y. SMYRLIS, *Implicit-explicit BDF methods for the Kuramoto-*
240 *Sivashinsky equation*, Appl. Numer. Math., 51 (2004), pp. 151-169.
- 241 4. M. ANITESCU, F. PAHLEVANI, AND W. LAYTON, *Implicit for local effects and explicit*
242 *for nonlocal effects is unconditionally stable*, Electron. Trans. Numer. Anal., 18 (2004),
243 pp. 174-187.
- 244 5. U. ASCHER, S. RUUTH, AND B. WETTON, *Implicit-explicit methods for time-dependent*
245 *partial differential equations*, SIAM J. Numer. Anal., 32 (1995), pp. 797-823.
- 246 6. G. BEAVERS AND D. JOSEPH, *Boundary conditions at a naturally permeable wall*, J. Fluid
247 Mech., 30 (1967), pp. 197-207.
- 248 7. Y. BOUBENDIR AND S. TLUPOVA, *Domain Decomposition Methods for Solving Stokes-*
249 *Darcy Problems with Boundary Integrals*, SIAM J. Sci. Comput., 35(1) (2013), pp. B82-
250 B106.
- 251 8. Y. CAO, M. GUNZBURGER, F. HUA, AND X. WANG, *Coupled Stokes-Darcy Model with*
252 *Beavers-Joseph Interface Boundary Condition*, Comm. Math. Sci., 8 (2010), pp. 1-25.
- 253 9. Y. CAO, M. GUNZBURGER, B. HU, F. HUA, X. WANG, AND W. ZHAO, *Finite element ap-*
254 *proximation of the Stokes-Darcy flow with Beavers-Joseph interface boundary condition*,
255 SIAM J. Num. Anal., 47 (2010), pp. 4239-4256.
- 256 10. Y. CAO, M. GUNZBURGER, X. HE AND X. WANG, *Robin-Robin Domain decomposition*
257 *method for Stokes-Darcy model with Beaver-Joseph interface condition*, Numer. Math.,
258 117 (2011), pp. 601-629.
- 259 11. Y. CAO, M. GUNZBURGER, X. HE AND X. WANG, *Parallel, non-iterative, multi-physics*
260 *domain decomposition methods for time-dependent Stokes-Darcy systems*, Math. Comp.,
261 S 0025-5718 (2014) 02779-8.
- 262 12. A. CESMELIOGLU, V. GIRAULT AND B. RIVIERE. *Time-dependent coupling of Navier-*
263 *Stokes and Darcy flows*, ESAIM Math. Model. Numer. Anal., doi:10.1051/m2an/2012034.
- 264 13. J. CHEN, S. SUN AND X.P. WANG. *A numerical method for a model of two-phase flow*
265 *in a coupled free flow and porous media system*, J Comput. Phys., 268(2014), pp. 1-16.
- 266 14. W. CHEN, P. CHEN, M. GUNZBURGER AND N. YAN, *Superconvergence analysis of FEMs*
267 *for the Stokes-Darcy System*, Math. Meth. the Appl. Sci., 33 (2010), pp. 1605-1617.
- 268 15. W. CHEN, M. GUNZBURGER, F. HUA, AND X. WANG, *A parallel Robin-Robin domain*
269 *decomposition method for the Stokes-Darcy system*, SIAM J. Numer. Anal., 49 (2011),
270 pp. 1064-1084.
- 271 16. W. CHEN, M. GUNZBURGER, D. SUN, AND X. WANG, *Efficient and long-time accurate*
272 *second order methods for Stokes-Darcy system*, SIAM Journal of Numerical Analysis,
273 51(5)2013, pp. 2563-2584.
- 274 17. P. CHARLET, *The Finite Element Method for Elliptic Problems*, North-Holland, Amster-
275 dam, 1978.
- 276 18. M. DISCACCIATI, E. MIGLIO, AND A. QUARTERONI, *Mathematical and numerical models*
277 *for coupling surface and groundwater flows*, Appl. Num. Math., 43 (2002), pp. 57-74.
- 278 19. M. DISCACCIATI AND A. QUARTERONI, *Analysis of a domain decomposition method for*
279 *the coupling of Stokes and Darcy equations*, In Numerical Mathematics and Advanced
280 Applications-ENUMATH 2001, F. Brezzi et al., eds, pp. 3-20, Springer-Verlag, Milan,
281 2003.
- 282 20. M. DISCACCIATI, A. QUARTERONI, AND A. VALLI, *Robin-Robin domain decomposition*
283 *methods for the Stokes-Darcy coupling*, SIAM J. Num. Anal., 45 (2007), pp. 1246-1268.
- 284 21. M. DISCACCIATI AND A. QUARTERONI, *Navier-Stokes/Darcy coupling: modeling, analy-*
285 *sis and numerical approximation*, Rev. Mat. Complut., 22(2) (2009), pp. 315-426.
- 286 22. V.J. ERVIN, E.W. JENKINS AND H. LEE, *Approximation of the Stokes-Darcy system by*
287 *optimization*, J. Sci. Comput., 59(3) (2014), pp. 775-794.
- 288 23. W. FENG, X. HE, Z. WANG AND X. ZHANG, *Non-iterative domain decomposition meth-*
289 *ods for a non-stationary Stokes-Darcy model with Beavers-Joseph interface condition*,
290 Appl. Math. Comput., 219(2) (2012), pp. 453-463.
- 291 24. J. FRANK, W. HUNSDORFER, AND J. VERWER, *Stability of implicit-explicit linear mul-*
292 *tistep methods*, Appl. Numer. Math., 25 (1996), pp. 193-205.
- 293 25. J. GALVIS AND M. SARKIS, *Non-matching mortar discretization analysis for the coupling*
294 *Stokes-Darcy equations*, Electron. Trans. Numer. Anal., 26 (2007), pp. 350-384.

- 295 26. V. GIRAULT AND P.A. RAVIART, *Finite Element Methods for Navier-Stokes Equations:*
296 *Theory and Algorithms*, Springer-Verlag, Berlin, 1986
- 297 27. R. GLOWINSKI, T. PAN, AND J. PERIAUX, *A Lagrange multiplier/fictitious domain*
298 *method for the numerical simulation of incompressible viscous flow around moving grid*
299 *bodies: I. Case where the rigid body motions are known a priori*, C. R. Acad. Sci. Paris
300 S er. I Math., 324 (1997), pp. 361-369.
- 301 28. E. HAIRER AND G. WANNER, *Solving Ordinary Differential Equations II: Stiff and*
302 *Differential-Algebraic Problems* 2nd ed, Springer-Verlag, Berlin, 2002.
- 303 29. A. HILL AND E. S ULI, *Approximation of the global attractor for the incompressible*
304 *Navier-Stokes equations*, IMA J. Num. Anal., 20 (2000), pp. 633-667.
- 305 30. W. J AGER AND A. MIKELIĆ, *On the interface boundary condition of Beavers, Joseph*
306 *and Saffman*, SIAM J. Appl. Math., 60 (2000), pp. 1111-1127.
- 307 31. I. JONES, *Low Reynolds number flow past a porous spherical shell*, Proc. Camb. Phil.
308 Soc., 73 (1973), pp. 231-238.
- 309 32. T. KINCAID, *Exploring the Secrets of Wakulla Springs*, Open Seminar, Tallahassee,
310 2004.
- 311 33. M. KUBACKI, *Uncoupling Evolutionary Groundwater-Surface Water Flows Using the*
312 *Crank-Nicolson Leapfrog Method*, Numer. Methods Partial Differential Eq., 29(4) (2013),
313 pp. 1192-1216.
- 314 34. E. KUNIANSKY, *U.S. Geological Survey Karst Interest Group Proceedings*, U.S. Geolog-
315 ical Survey Scientific Investigations Report, Bowling Green, pp. 2008-5023, 2008.
- 316 35. W. LAYTON, F. SCHIEWECK, AND I. YOTOV, *Coupling fluid flow with porous media flow*,
317 SIAM J. Num. Anal., 40 (2003), pp. 2195-2218.
- 318 36. W. LAYTON, H. TRAN, AND C. TRENCH, *Analysis of long time stability and errors*
319 *of two partitioned methods for uncoupling evolutionary groundwater-surface water flows*,
320 SIAM J. Numer. Anal., 51(1) (2013), pp. 248-272.
- 321 37. W. LAYTON, H. TRAN AND X. XIONG, *Long time stability of four methods for splitting*
322 *the evolutionary Stokes-Darcy problem into Stokes and Darcy subproblems*, J. Comput.
323 Appl. Math., 236 (2012), pp. 3198-3217.
- 324 38. W.J. LAYTON AND C. TRENCH, *Stability of two IMEX methods, CNLF and BDF2-*
325 *AB2, for uncoupling systems of evolution equations*, Appl. Numer. Math., 62 (2012),
326 pp. 112-120.
- 327 39. H. LEE AND K. RIFE, *Least squares approach for the time-dependent nonlinear Stokes-*
328 *Darcy flow*, Math. Method Appl. Sci., 67(10) (2014), pp. 1806-1815.
- 329 40. A. M ARQUEZ, S. MEDDAHI AND F.J. SAYAS, *A decoupled preconditioning technique for*
330 *a mixed Stokes-Darcy model*, J. Sci. Comput., 57(1) (2013), pp. 174-192.
- 331 41. M. MU AND J. XU, *A two-grid method of a mixed Stokes-Darcy model for coupling fluid*
332 *flow with porous media flow*, SIAM J. Numer. Anal., 45 (2007), pp. 1801-1813.
- 333 42. M. MU AND X. ZHU, *Decoupled schemes for a non-stationary mixed Stokes-Darcy model*,
334 *Math. Comp.*, 79 (2010), pp. 707-731.
- 335 43. A. QUARTERONI AND A. VALLI, *Domain Decomposition Methods for Partial Differential*
336 *Equations*, Oxford Science Publications, Oxford, 1999.
- 337 44. P. SAFFMAN, *On the boundary condition at the interface of a porous medium*, Stud. in
338 Appl. Math., 1 (1971), pp. 77-84.
- 339 45. L. SHAN, H. ZHENG, AND W. LAYTON, *A decoupling method with different subdomain*
340 *time steps for the nonstationary Stokes-Darcy model*, Numer. Meth. Part. D. E., 29(2)
341 (2013), pp. 549-583.
- 342 46. L. SHAN AND H. ZHENG, *Partitioned Time Stepping Method for Fully Evolutionary*
343 *Stokes-Darcy Flow with Beavers-Joseph Interface Conditions*, SIAM J. Numer. Anal.,
344 51(2) (2013), pp. 813-839.
- 345 47. Z. SI, Y. WANG AND S. LI, *Decoupled modified characteristics finite element method for*
346 *the time dependent Navier-Stokes/Darcy problem*, Math. Method Appl. Sci., 37(9) (2014),
347 pp. 1392-1404.
- 348 48. L. ZUO AND Y. HOU, *A decoupling two-grid algorithm for the mixed Stokes-Darcy model*
349 *with the Beavers-Joseph interface condition*, Numer. Meth. Part. D. E., 30(3) (2014),
350 pp. 1066-1082.